Original Article

eISSN 2765-205X
Organoid 2023;3:e3 • https://doi.org/10.51335/organoid.2023.3.e3

Organoid

One-step achievement of tumor spheroid-induced angiogenesis in a high-throughput microfluidic platform: one-step tumor angiogenesis platform

Seonghyuk Park[1,*], Youngtaek Kim[1,*], Jihoon Ko[1,2], Jiyoung Song[1], Jeeyun Lee[2,3], Young-Kwon Hong[4], Noo Li Jeon[1,5,6]

[1]Department of Mechanical Engineering, Seoul National University, Seoul, Korea
[2]Division of Hematology-Oncology, Department of Medicine, Samsung Medical Center, Sungkyunkwan University School of Medicine, Seoul, Korea
[3]Department of Health Sciences and Technology, Samsung Advanced Institute for Health Science and Technology, Sungkyunkwan University, Seoul, Korea
[4]Department of Surgery, Norris Comprehensive Cancer Center, Keck School of Medicine, University of Southern California, Los Angeles, CA, USA
[5]Institute of Advanced Machinery and Design, Seoul National University, Seoul, Korea 6 Institute of Bioengineering, Seoul National University, Seoul, Korea

Received: August 19, 2022
Revised: December 12, 2022
Accepted: December 19, 2022

Correspondence to:
Noo Li Jeon, PhD
Department of Mechanical Engineering, Seoul National University, 1 Gwanak-ro, Gwanak-gu, Seoul 08826, Korea
E-mail: njeon@snu.ac.kr

*These authors contributed equally.

Research on the development of anti-cancer drugs has progressed, but the low reliability of animal experiments due to biological differences between animals and humans causes failures in the clinical process. To overcome this limitation, 3-dimensional (3D) *in vitro* models have been developed to mimic the human cellular microenvironment using polydimethylsiloxane (PDMS). However, due to the characteristics and limitations of PDMS, it has low efficiency and is not suitable to be applied in the preclinical testing of a drug. High-throughput microfluidic platforms fabricated by injection molding have been developed, but these platforms require a laborious process when handling spheroids. We recently developed an injection-molded plastic array 3D culture tissue platform that integrates the process from spheroid formation to reconstruction of an *in vitro* model with spheroids (All-in-One-IMPACT). In this study, we implemented a 3D tumor spheroid angiogenesis model in the developed platform. We analyzed the tendency for angiogenesis according to gel concentration and confirmed that angiogenesis occurred using cancer cell lines and patient-derived cancer cells (PDCs). We also administered an anti-cancer drug to the PDC tumor spheroid angiogenesis model to observe the drug's effect on angiogenesis according to its concentration. We demonstrated that our platform can be used to study the tumor microenvironment (TME) and drug screening. We expect that this platform will contribute to further research on the complex mechanisms of the TME and predictive preclinical models.

Keywords: Microfluidics; Mircophysiological system; Angiogenesis; Tumor microenvironment; Drug screening

Introduction

Various factors that threaten human health and prosperity exist, among which diseases are especially prominent [1]. In particular, cancer is a disease that endangers human life. Despite research to overcome cancer, it still accounts for a large proportion of deaths in humans [2]. To develop drugs and therapies for cancer treatment, it is necessary to consider whether drugs and therapies are effective when used in humans, whether there are side effects, and whether other unexpected mechanisms may occur [3–5]. However, it is quite challenging to develop an optimal treatment through the process. Generally, animal experiments have been conducted for drug development and preclinical verification [6–8].

However, the results obtained from animal experiments have low reliability for humans due to the biological differences between humans and animals [9,10]. Indeed, most drugs in the development process fail to pass clinical trials, and the failure of drug development causes an enormous waste of money, time, and personnel [11].

To solve the limitations of animal experiments, *in vitro* models that mimic the human body environment have emerged. In previous *in vitro* models, 2-dimensional (2D) cell culture models based on human cells were developed to overcome biological differences [12,13]. However, it is difficult to mimic 3D structures, which results in morphological differences between models and the *in vivo* setting [14]. To overcome these limitations, many groups have studied models that mimic the 3D microenvironment of the human body. Organs-on-a-chip have been developed to construct 3D *in vitro* models of human tissues and organs through microfluidics [15–17]. Polydimethylsiloxane (PDMS) has typically been used to fabricate these platforms, but there are limitations due to the characteristics of the material [18,19]. For instance, the high cost of fabricating these platforms results in low experimental efficiency. Since high-throughput experiments for various conditions are required to develop cancer treatment, these limitations should be overcome.

Our research group has developed an injection-molded microfluidic platform to overcome the limitations of PDMS, enabling the construction of 3D *in vitro* models, including the tumor microenvironment (TME) [20–23]. This platform solves previous issues of material properties, but it also has problems in efficiency, especially for introducing cancer spheroids. To inject and culture spheroids in the platform, it is necessary to extract spheroids that were cultured in a separate platform (e.g., a U-shaped 96-well plate) through a pipette. Furthermore, a process of mixing the spheroids with endothelial cells, stromal cells and hydrogel, and then patterning the mixture to match the platform is required to reconstruct the TME [24,25]. Through these laborious steps, some spheroids might be damaged or missed, reducing the reliability and efficiency of the experiments. To solve these issues, we have developed a novel microfluidic platform, All-in-One-IMPACT, which is designed to carry out the process from spheroid formation to reconstruction of the TME at once without requiring the user to perform technically difficult steps.

Biological applications using All-in-One-IMPACT in previous research have included the construction and validation of a vascularized tumor spheroid model. Through the research, we demonstrated the morphology of tumor spheroids and the blood vessels surrounding them. However, to reliably elucidate effects in the cancer-vascular co-culture environment, studies on angiogenesis should be performed [26]. Understanding the morphological aspect of angiogenic blood vessels co-cultured with cancer spheroids in the TME is crucial to show how similar the engineered *in vitro* model is to the *in vivo* microenvironment [27]. Therefore, we constructed a tumor spheroid angiogenesis model in the All-in-One-IMPACT platform without laborious steps. We observed angiogenesis according to the concentration of the hydrogel constituting the TME and various types of tumor spheroids in specific concentrations of the hydrogel. We also observed how angiogenesis was changed when an anti-angiogenic drug was administered to a spheroid angiogenesis model of patient-derived cancer cells (PDCs). We expect that the platform developed through this study could be used for further studies of the TME and cancer treatment.

Materials and Methods

Ethics statement: This study was approved by the Institutional Review Board (IRB) of Samsung Medical Center (IRB no. #202109052). Informed consent was obtained using the opt-out method.

1. Device design and fabrication

The design of All-in-One-IMPACT and the reproducibility of its patterning were verified with a 3D printer (3D Systems, Rock Hill, SC, USA). The optimized design was fabricated by injection molding with polystyrene (PS) (R&D Factory, Hwaseong, Korea). The aluminum alloy core mold used for the injection molding was machined by a milling machine (Fanuc, Oshino, Japan). In preparation for the experiment, the PS platform was

treated with O_2 plasma (Femto, Hwaseong, Korea) for 10 minutes and then put it in a 60°C oven for 7 days. For the experiment, single-sided pressure-sensitive adhesive film was attached to the bottom side of the platform. The prototype fabricated by the 3D printer and the alloy mold core were designed using Solidworks (Dassault Systèmes, Vélizy-Villacoublay, France).

2. Cell preparation

Human lung fibroblasts (LFs; Lonza, Hayward, CA, USA), A549, HEPG2, U87MG cells (Korean Cell Line Bank, Seoul, Korea), and gastric cancer PDCs were used to form spheroids in the platform. To reconstruct the 3D TJE, we used human umbilical vein endothelial cells (HUVECs; Lonza) and LFs. Cancer cell lines and PDCs were cultured in RPMI 1640 supplemented with 10% fetal bovine serum (HyClone; Logan, UT, USA) and 1% penicillin-streptomycin (Gibco; Waltham, MA, USA). HUVECs were cultured in endothelial growth medium 2 (EGM-2; Lonza) and LFs were cultured in fibroblast growth medium 2 (Lonza). The cells were incubated in a 5% CO_2 humidified incubator at 37°C.

3. Formation of tumor spheroids

To form tumor spheroids in All-in-One-IMPACT, A549 cells, HEPG2, U87MG, PDCs, and LFs were used. We mixed LF and tumor cell suspensions as a 1:1 ratio and then loaded them into the platform. To obtain sufficient and necessary conditions for spheroid formation, we kept the platform in the incubator for a day.

4. Construction of a 3D tumor spheroid angiogenesis model

To develop a tumor angiogenesis model in All-in-One-IMPACT, we mixed the LF suspension and fibrinogen (Sigma-Aldrich; St. Louis, MO, USA) as a 1:1 ratio and then loaded 3 L of the mixture into the center channel of the platform. After 12 minutes to solidify the suspension gel, we attached HUVECs to the channels on both sides (10 each). As inhibitors, we dissolved axitinib, bevacizumab, and sunitinib in dimethyl sulfoxide (Sigma-Aldrich) and diluted the mixtures serially into 4 concentrations (axitinib: 0.01 nM, 0.1 nM, 1.0 nM, and 10 nM; bevacizumab: 0.01 mg/mL, 0.1 mg/mL, 1.0 mg/mL, and 10 mg/mL; sunitinib: 0.01 μM, 0.1 μM, 1.0 μM, and 10 μM). Each drug was introduced via EGM-2 medium.

5. Immunocytochemistry

The samples were fixed with 4% paraformaldehyde (Biosesang, Seongnam, Korea) for 15 minutes and washed with phosphate-buffered saline (Gibco). To permeabilize the samples, we administered 0.2% Triton X-100 (Sigma-Aldrich) for 30 minutes, and then treated the samples with 3% bovine serum albumin (BSA; Millipore, Billerica, MA, USA) for 2 hours. To stain endothelial and tumor cells, we used 488 Ulex europaeus agglutinin 1 (Vector Laboratories, Burlington, MA, USA) and Alexa Fluor 594-tagged variants of anti-epithelial cell adhesion molecule (BioLegend, San Diego, CA, USA) at a 1:500 ratio in BSA for 2 days. We used a confocal microscope (Nikon Ti 2; Nikon, Tokyo, Japan) to image the stained samples.

6. Statistical image analysis

We converted 3D confocal images to 2D images by z-projection, then cropped the region of interest. The vessel area was directly measured using ImageJ (National Institutes of Health) and the angiogenic junction was measured using Angiotool (National Cancer Institute). A statistical comparison of the analyzed data was performed with Prism ver. 8 (GraphPad, San Diego, CA, USA) using the unpaired two-tailed Student t-test. The p-value thresholds for statistical significance were set as $^{*}p<0.1$, $^{**}p<0.01$, $^{***}p<0.001$.

Results and Discussion

1. Schematic of the platform and the experiment

We used an injection-molded microfluidic platform that integrates the process from spheroid formation to vascularization (All-in-One-IMPACT, Fig. 1A). The platform has the format of a 96-well plate and the size of a slide glass (1 inch 3 inches). The platform has 8 identical wells, each of which consists of 2 parts: a spheroid formation area and a cell culture region [28]. Both parts are designed to pattern a liquid for spheroid formation and reconstruction of the 3D microenvironment. We demonstrated that the liquid was well patterned using a prototype fabricated by a 3D printer (Fig. 1B).

The integrated process of the platform is described as follows (Fig. 1C). In the spheroid formation area, a cell culture medium including cells for spheroid formation (e.g., targeted cells for spheroid and fibroblast cells) was injected into the platform. Then, the liquid formed a droplet at the end point of the spheroid formation area. After 24 hours, cells aggregated to the droplet and a spheroid was achieved. In the cell culture area, a 200-m tall microchannel is under the spheroid formation area. Components such as hydrogel and cells were injected into the microchannel, and the platform was maintained in the cell culture incubator. After a few days of cell culture, the 3D microenvironment with spheroids was constructed in the platform.

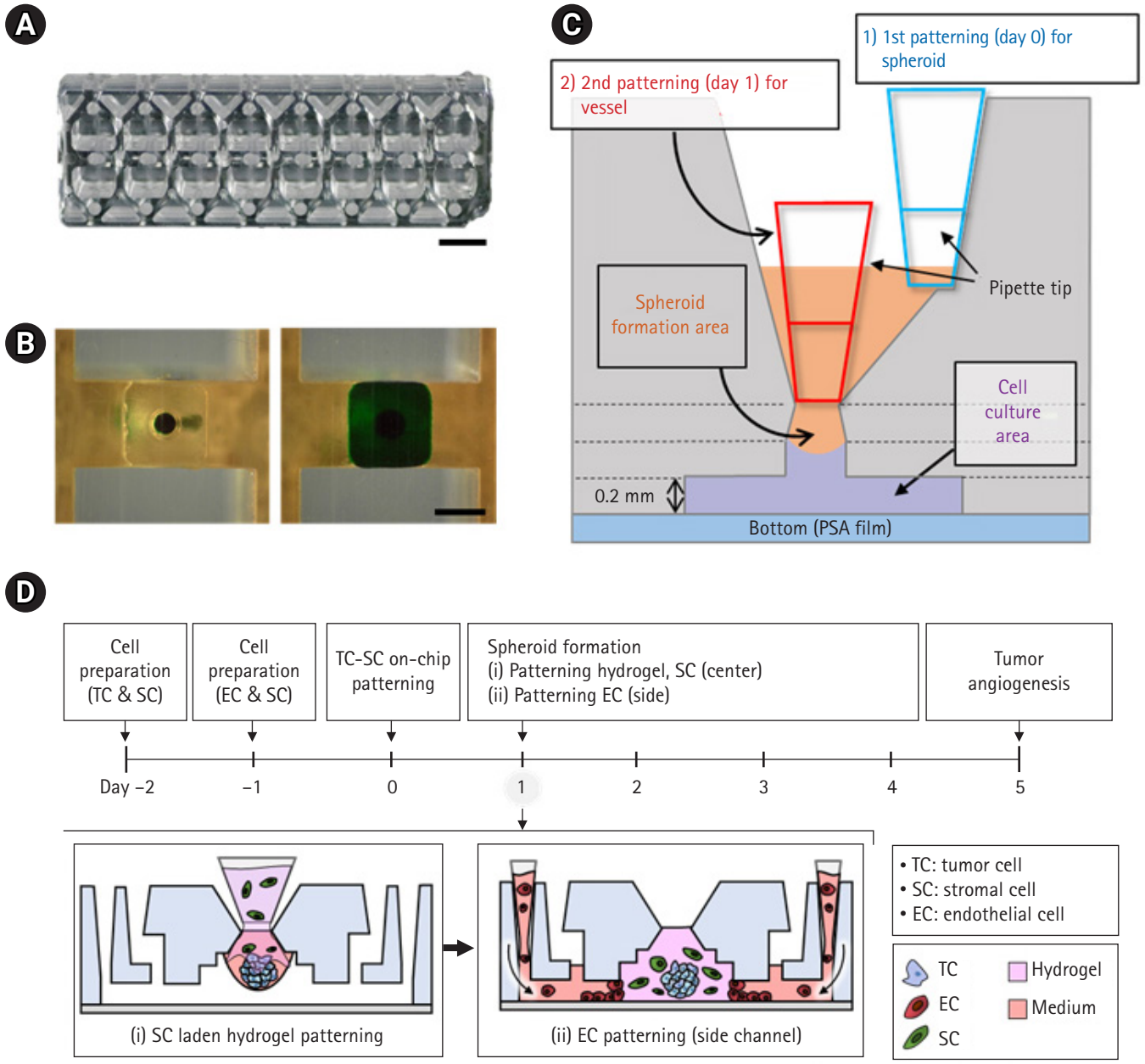

Fig. 1. Schematic diagram of All-in-One-IMPACT. (A) Photograph of All-in-One-IMPACT fabricated by injection molding. Scale bar=2 mm. (B) Liquid patterning in the prototype of All-in-One-IMPACT fabricated by a 3-dimensional printer. Scale bar=2 mm. (C) Design and parts of All-in-One-IMPACT. Pressure-sensitive adhesive film is attached to the bottom of polystyrene-based body. The platform consists of (i) a spheroid formation area and (ii) a cell culture area. (D) The cell culture protocol for tumor angiogenesis in All-in-One-IMPACT. (i) Patterning of fibroblasts with hydrogel at the center channel and (ii) attaching ECs to the hydrogel interface to induce angiogenic sprouting. PSA, pressure sensitive adhesion.

With this design of the platform, we performed experiments to model 3D tumor spheroid angiogenesis (Fig. 1D). We planned to generate tumor spheroids and inject a hydrogel with stromal cells in order to attach endothelial cells for angiogenesis at both sides of the microchannel.

2. 3D tumor spheroid angiogenesis models for hydrogel conditions

First, we observed tumor spheroid angiogenesis according to hydrogel conditions. We especially focused on gel concentration to clarify whether it affects angiogenesis with tumor spheroids. We chose fibrin gel, which is generally used for modeling *in vitro* 3D

vascular networks, and performed experiments using 4 concentrations (1.25 mg/mL, 2.5 mg/mL, 5 mg/mL, and 10 mg/mL) of fibrin gel and control (2.5 mg/mL without tumor spheroids) to construct angiogenesis models. For tumor spheroids, we used gastric cancer PDCs that were used in the previous study [28]. Through the sample images that were obtained from confocal microscopy, we observed that tumor spheroid angiogenesis in 2.5 mg/mL fibrin gel showed the most sprouted vascular network compared to other concentrations and the control group (Fig. 2A). A possible explanation might be that tumor spheroids induced angiogenic effects on endothelial cells. Regarding other concentrations, angiogenesis in a 1.25 mg/mL concentration of the gel also showed a well-formed vascular network. However, angiogenesis in 5 mg/mL and 10 mg/mL concentrations of fibrin gel showed unaligned, unstable, and short vascular networks.

We quantitatively analyzed tumor spheroid angiogenesis using Angiotool and plotted graphs according to the end-point,

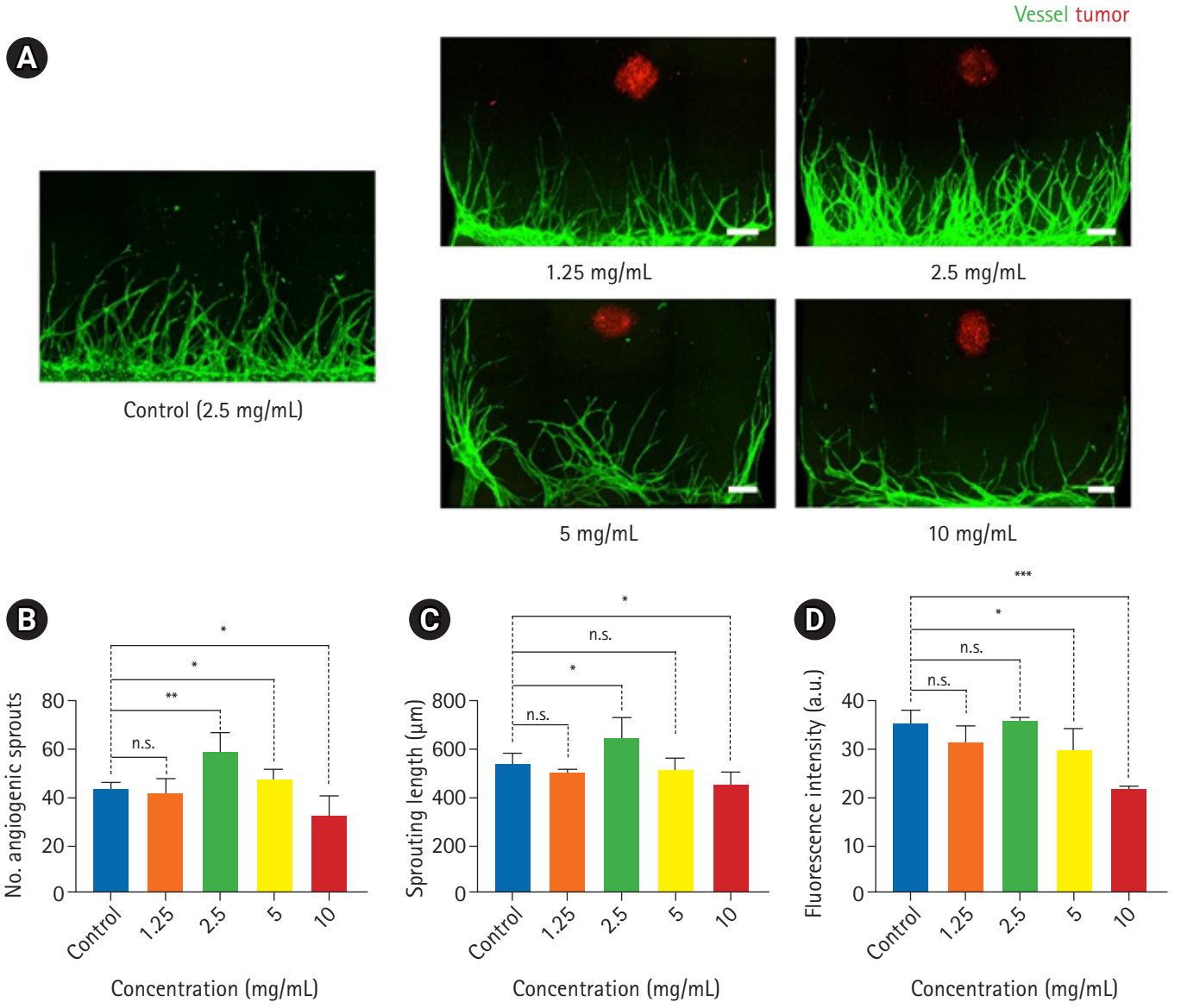

Fig. 2. Three-dimensional tumor angiogenesis for 4 different gel concentrations in All-in-One-IMPACT. (A) Confocal fluorescence images show distinct morphology of angiogenic sprouts for 4 days under co-culture conditions with patient-derived gastric cancer cells (PDCs) at different fibrin gel concentrations. Scale bar=250 m. Cancer cells were stained with EpCAM 594 (red) and endothelial cells were stained with lectin 488 (green). (B-D) Quantitative analysis of the number of angiogenic sprouts, sprouting length, and fluorescence intensity for each gel concentration. n=8 per each condition. ns, no significance. The p-value thresholds for statistical significance were set as *p<0.1, **p<0.01, ***p<0.001.

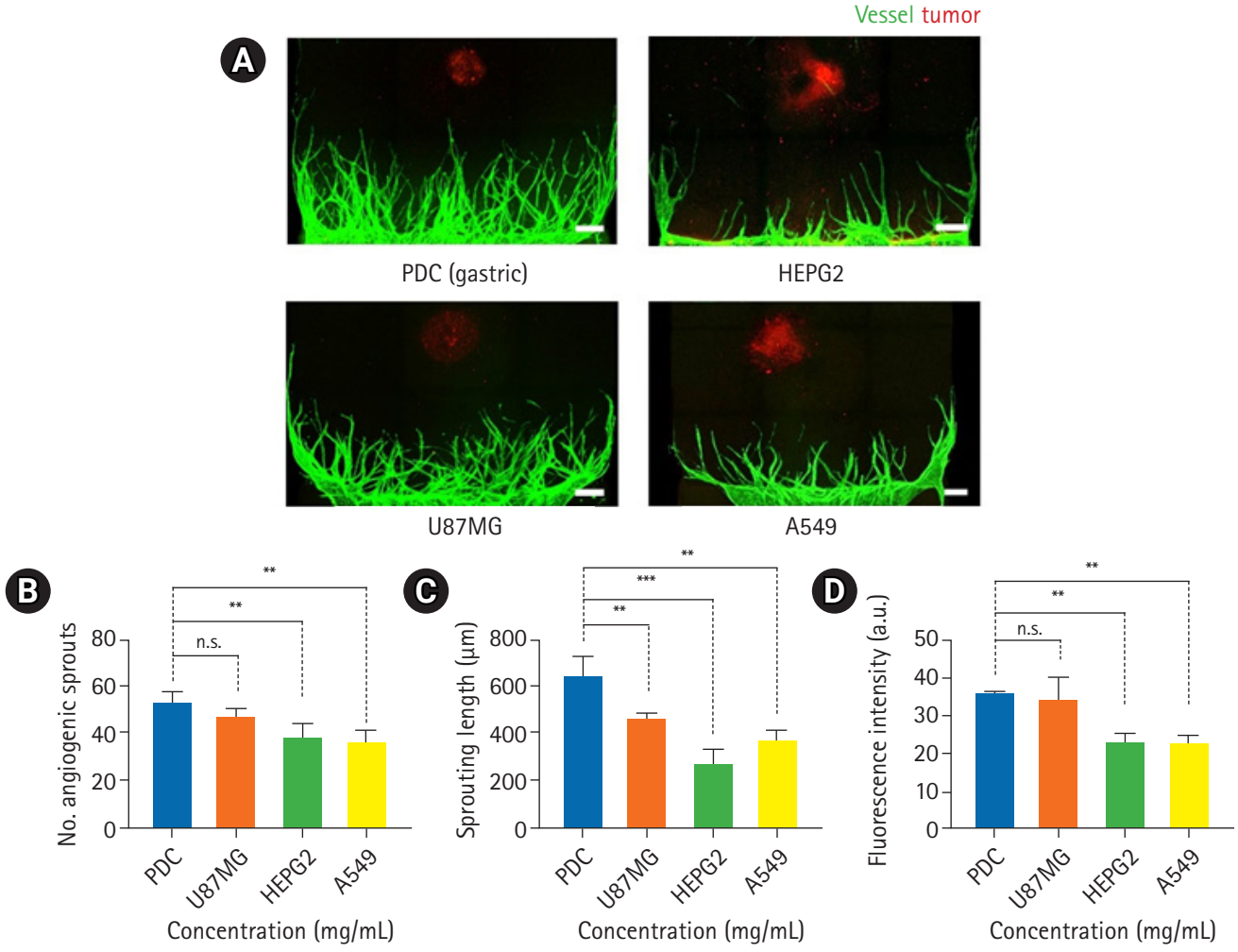

Fig. 3. Three-dimensional tumor angiogenesis for 4 cancer cell types in All-in-One-IMPACT. (A) Confocal fluorescence images show distinct morphology of angiogenic sprouts for 4 days under co-culture conditions with 4 types of cancer cells (PDC, HEPG2, U87MG, A549) and a 2.5 mg/mL gel concentration. Scale bar=250 m. Cancer cells were stained with EpCAM 594 (red) and endothelial cells were stained with lectin 488 (green). (B-D) Quantitative analysis of the number of angiogenic sprouts, sprouting length, and fluorescence intensity for each type of cancer cell. n=8 per each condition. ns, no significance. The p-value thresholds for statistical significance were set as *p<0.1, **p<0.01, ***p<0.001.

sprouting length, and vascular area (Fig. 2B–D). Similar to the morphological data in Fig. 2A, angiogenesis in a 2.5 mg/mL gel concentration showed a higher values for all metrics than were observed in other conditions. Furthermore, in a 1.25 mg/mL concentration of gel, the graphs showed similar values to the control data for all metrics. However, angiogenesis in a 5 mg/mL gel concentration showed similar values to the control and 1.25 mg/mL data. This demonstrated that despite high quantitative values for sprouting and culturing of the vascular network, the alignment and shape of the network could be unstable and difficult to view as well-formed angiogenesis. Finally, in a 10 mg/mL gel concentration, lower values were found for all metrics. An explanation for this might be that a high concentration of hydrogel has a dense structure that makes it difficult for endothelial cells to invade and sprout as the vascular network.

The experiment in this study was limited in scope to analyzing changes according to the concentration of hydrogel. In a more elaborate study on angiogenesis, experiments with various hydrogels (e.g. collagen gel or Matrigel) are also required. Since the extracellular matrix (ECM) is a crucial component in the TME and the hydrogel in an *in vitro* model plays the role of the ECM in TME, further studies on various conditions of the hydrogel should be performed.

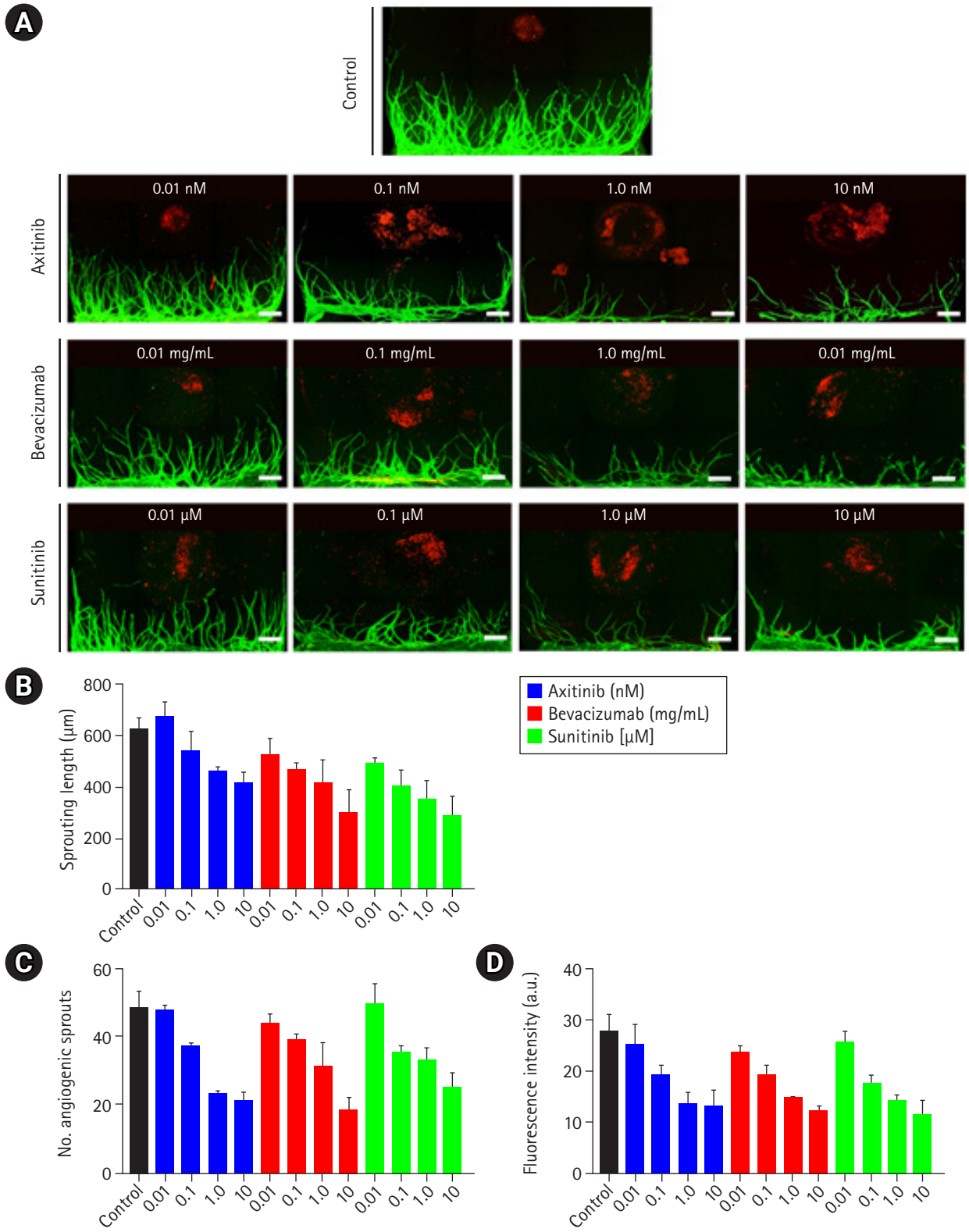

Fig. 4. Screening of the efficacy of anti-cancer drugs for inhibiting tumor angiogenesis in All-in-One-IMPACT. The conditions for drug screening for angiogenesis were selected as patient-derived gastric cancer cells (PDCs) and 2.5 mg/mL of fibrin gel. Serially diluted drugs (axitinib, bevacizumab, and sunitinib) were administered via the medium on day 2 and incubated for 2 days. (A) Confocal fluorescence images show a dose-dependent drug effect for tumor angiogenic sprouting. Scale bar=500 μm. Cancer cells were stained with EpCAM 594 (red) and endothelial cells were stained with lectin 488 (green). (B-D) Quantitative analysis of the number of angiogenic sprouts, sprouting length, and fluorescence intensity for each dose of drugs. n=8 per each condition.

3. Various types of tumor spheroid angiogenesis models

After observing tumor spheroid angiogenesis in the hydrogel, we constructed tumor spheroid angiogenesis models with various types of tumor cells. As we demonstrated that the most robust angiogenesis was generated in a 2.5 mg/mL concentration of fibrin gel, as discussed in section 3.2., we chose a fibrin gel concentration of 2.5 mg/mL in the experiment. We used cancer cell lines, including HEPG2, U87MG, and A549, and gastric cancer PDCs for tumor spheroids. We obtained images using confocal microscopy, as described in section 3.2., and observed the sample images (Fig. 3A). Compared to PDCs, angiogenesis with U87MG spheroids was well generated, whereas less angiogenesis was observed for HEPG2 and A549 cells.

We also plotted graphs using assays identical to those described in section 3.2. for a quantitative comparison according to tumor cell type (Fig. 3B–D). For end-point and sprouting length, U87MG showed slightly lower values and HEPG2 and A549 showed intensely lower values than were observed for PDCs. An explanation for this could be that PDCs had characteristics that induced a stronger angiogenic effect on endothelial cells than was observed for cancer cell lines. Moreover, there are differences between each tumor cell type that could have affected angiogenesis. For the vascular area, U87MG showed similar values to PDCs, while and HEPG2 and A549 showed lower values. Further studies are necessary to classify and analyze the differences among various types of tumor spheroids, including proteomic and genomic characteristics, which were not investigated in this study.

4. Drug treatment in 3D tumor spheroid angiogenesis models

To show the possibility of using the platform for drug screening in relation to the TME, we administered drugs to the tumor spheroid angiogenesis models constructed in All-in-One-IMPACT. We chose the conditions where the most stable vascular network was formed in previous experiments: 2.5 mg/mL of fibrin gel and tumor spheroids from PDCs. We used axitinib and sunitinib as inhibitors of vascular endothelial growth factor (VEGF) receptor and bevacizumab as an inhibitor of VEGF, and set concentrations to 4 ranges (axitinib: 0.01 nM, 0.1 nM, 1.0 nM, and 10 nM; bevacizumab: 0.01 mg/mL, 0.1 mg/mL, 1.0 mg/mL, and 10 mg/mL; sunitinib: 0.01 μM, 0.1 μM, 1.0 μM, and 10 μM) (Fig. 4A). As shown in the sample images, we observed that in all conditions, except 0.01 nM axitinib, angiogenesis was weakened compared to control. Over a specific concentration (0.1 nM in this study), axitinib exerted an anti-angiogenic effect on the model. Of particular note, all tumor spheroids in each condition collapsed or were separated. Further research demonstrating the effects of anti-angiogenic drugs on tumor spheroids will be required, although it was beyond the scope of this study.

Through the plotted graphs using data from the angiogenesis assay, we observed a tendency for lower values in all 3 metrics under all conditions, except 0.01 nM axitinib, than in the control group (Fig. 4B–D). Bevacizumab showed the greatest effect on angiogenesis compared to the other drugs at the highest concentration. As with the morphological data, an explanation for these findings could be that the drugs exerted anti-angiogenic effects in this model of angiogenesis that were proportional to their concentrations.

In conclusion, we presented a novel microfluidic plastic array cell culture platform, All-in-One-IMPACT, that integrates spheroid formation and reconstruction of the TME. Previously, an additional platform (e.g., a well plate) was used to form spheroids, and a user-dependent, laborious process was required to use the platform. Using the developed platform, we reduced the complexity of the experimental process and facilitated spheroid formation and hydrogel patterning. We performed 3D tumor spheroid angiogenesis using the platform to study an *in vitro* TME model. We analyzed the effect of the hydrogel concentration on angiogenesis during co-culture. The gel concentration is one of the conditions used to reconstruct TME, and we confirmed that the tendency for angiogenesis varied depending on the concentration of hydrogel. Also, we observed angiogenesis with tumor spheroids of various cell lines and PDCs. Finally, with the optimized gel concentration and cancer cell type, we treated the angiogenesis model with anti-angiogenic drugs and analyzed the morphology of the blood vessels. Through this study, we demonstrated that our platform could effectively be used for *in vitro* cancer research. We expect that All-in-One-IMPACT will contribute to further TME research and drug development.

Notes

Conflict of interest

No potential conflict of interest relevant to this article was reported.

Funding

This work was supported by the National Research Foundation of Korea (NRF; Grant No. NRF-2021R1A3B1077481). This research was financially supported by the Ministry of Trade, Industry and Energy (MOTIE) and the Korea Institute for

Advancement of Technology (KIAT) through the International Cooperative R&D program (P0011266).

Author contributions

Conceptualization: SP, YK, NLJ; Visualization: SP, YK; Investigation: SP, YK, JK; Supervision: NLJ; Validation: J Ko, JS, JL, YKH, NLJ; Writing-original draft: SP, YK; Writing-review & editing: all authors.

ORCID

Seonghyuk Park, https://orcid.org/0009-0004-8946-1993
Youngtaek Kim, https://orcid.org/0000-0002-4654-5925
Jihoon Ko, https://orcid.org/0000-0002-6555-3728
Jeeyun Lee, https://orcid.org/0000-0002-4911-6165
Young-Kwon Hong, https://orcid.org/0000-0001-8245-875X
Noo Li Jeon, https://orcid.org/0000-0003-0490-3592

Data availability

Please contact the corresponding author for data availability.

References

1. Murphy SL, Xu J, Kochanek KD, Curtin SC, Arias E. Deaths: final data for 2012. Natl Vital Stat Rep 2013;61:1–168.
2. Siegel RL, Miller KD, Fuchs HE, Jemal A. Cancer statistics, 2022. CA Cancer J Clin 2022;72:7–33.
3. Yap TA, Sandhu SK, Workman P, de Bono JS. Envisioning the future of early anticancer drug development. Nat Rev Cancer 2010;10:514–23.
4. Fortin S, Bérubé G. Advances in the development of hybrid anticancer drugs. Expert Opin Drug Discov 2013;8:1029–47.
5. Qi L, Luo Q, Zhang Y, Jia F, Zhao Y, Wang F. Advances in toxicological research of the anticancer drug cisplatin. Chem Res Toxicol 2019;32:1469–86.
6. Jung J. Human tumor xenograft models for preclinical assessment of anticancer drug development. Toxicol Res 2014;30:1–5.
7. Clarke R. The role of preclinical animal models in breast cancer drug development. Breast Cancer Res 2009;11(Suppl 3):S22.
8. Ruggeri BA, Camp F, Miknyoczki S. Animal models of disease: pre-clinical animal models of cancer and their applications and utility in drug discovery. Biochem Pharmacol 2014;87:150–61.
9. Van Norman GA. Limitations of animal studies for predicting toxicity in clinical trials: is it time to rethink our current approach? JACC Basic Transl Sci 2019;4:845–54.
10. Cekanova M, Rathore K. Animal models and therapeutic molecular targets of cancer: utility and limitations. Drug Des Devel Ther 2014;8:1911–21.
11. Seruga B, Ocana A, Amir E, Tannock IF. Failures in phase III: causes and consequences. Clin Cancer Res 2015;21:4552–60.
12. Li Y, Kilian KA. Bridging the gap: from 2D cell culture to 3D microengineered extracellular matrices. Adv Healthc Mater 2015;4:2780–96.
13. Kapałczyńska M, Kolenda T, Przybyła W, Zajączkowska M, Teresiak A, Filas V, et al. 2D and 3D cell cultures: a comparison of different types of cancer cell cultures. Arch Med Sci 2018;14:910–9.
14. Jensen C, Teng Y. Is it time to start transitioning from 2D to 3D cell culture? Front Mol Biosci 2020;7:33.
15. Ma C, Peng Y, Li H, Chen W. Organ-on-a-chip: a new paradigm for drug development. Trends Pharmacol Sci 2021;42:119–33.
16. Zheng F, Fu F, Cheng Y, Wang C, Zhao Y, Gu Z. Organ-on-a-chip systems: microengineering to biomimic living systems. Small 2016;12:2253–82.
17. Ahadian S, Civitarese R, Bannerman D, Mohammadi MH, Lu R, Wang E, et al. Organ-on-a-chip platforms: a convergence of advanced materials, cells, and microscale technologies. Adv Healthc Mater 2018;7:1700506.
18. Miranda I, Souza A, Sousa P, Ribeiro J, Castanheira EM, Lima R, et al. Properties and applications of PDMS for biomedical engineering: a review. J Funct Biomater 2021;13:2.
19. Guckenberger DJ, Berthier E, Young EW, Beebe DJ. Induced hydrophobic recovery of oxygen plasma-treated surfaces. Lab Chip 2012;12:2317–21.
20. Kim S, Ko J, Lee SR, Park D, Park S, Jeon NL. Anchor-IMPACT: a standardized microfluidic platform for high-throughput antiangiogenic drug screening. Biotechnol Bioeng 2021;118:2524–35.
21. Park D, Son K, Hwang Y, Ko J, Lee Y, Doh J, et al. High-throughput microfluidic 3D cytotoxicity assay for cancer immunotherapy (CACI-IMPACT Platform). Front Immunol 2019;10:1133.
22. Lee B, Kim S, Ko J, Lee SR, Kim Y, Park S, et al. 3D micromesh-based hybrid bioprinting: multidimensional liquid patterning for 3D microtissue engineering. NPG Asia Mater 2022;14:6.
23. Song J, Choi H, Koh SK, Park D, Yu J, Kang H, et al. High-throughput 3D in vitro tumor vasculature model for real-time monitoring of immune cell infiltration and cyto-

toxicity. Front Immunol 2021;12:733317.
24. Ko J, Ahn J, Kim S, Lee Y, Lee J, Park D, et al. Tumor spheroid-on-a-chip: a standardized microfluidic culture platform for investigating tumor angiogenesis. Lab Chip 2019;19:2822–33.
25. Shin N, Kim Y, Ko J, Choi SW, Hyung S, Lee SE, et al. Vascularization of iNSC spheroid in a 3D spheroid-on-a-chip platform enhances neural maturation. Biotechnol Bioeng 2022;119:566–74.
26. Mielgo A, Seguin L, Huang M, Camargo MF, Anand S, Franovic A, et al. A MEK-independent role for CRAF in mitosis and tumor progression. Nat Med 2011;17:1641–5.
27. Kwak TJ, Lee E. In vitro modeling of solid tumor interactions with perfused blood vessels. Sci Rep 2020;10:20142.
28. Kim Y, Ko J, Shin N, Park S, Lee SR, Kim S, et al. All-in-one microfluidic design to integrate vascularized tumor spheroid into high-throughput platform. Biotechnol Bioeng 2022;119:3678–93.